

# Yb<sup>3+</sup>,Er<sup>3+</sup>:YAG at high temperatures: Energy transfer and spectroscopic properties

B. Denker<sup>a</sup>, B. Galagan<sup>a</sup>, V. Osiko<sup>a</sup>, S. Sverchkov<sup>a</sup>, A.M. Balbashov<sup>b</sup>,  
J.E. Hellström<sup>c,\*</sup>, V. Pasiskevicius<sup>c</sup>, F. Laurell<sup>c</sup>

<sup>a</sup> *A.M.Prokhorov General Physics Institute, Vavilova Str 38, 119991 Moscow, Russia*

<sup>b</sup> *Moscow Power Engineering Institute, Moscow, Russia*

<sup>c</sup> *Department of Physics, Royal Institute of Technology, 10044 Stockholm, Sweden*

Received 17 March 2006; received in revised form 20 September 2006; accepted 20 September 2006

## Abstract

Energy transfer and spectroscopic properties at high temperatures have been investigated in Er,Yb:YAG crystals. It is shown that at elevated temperatures around 600–800 °C these characteristics become similar to those in the efficient 1.5 μm laser medium – Er,Yb-doped phosphate glasses.

© 2006 Elsevier B.V. All rights reserved.

## 1. Introduction

Er-doped bulk laser systems emitting in the 1.5 μm region meet significant interest since this wavelength region is considered eye-safe. For example, erbium bulk pulsed lasers operating in the Q-switched regime are very attractive for applications like LIDARs and rangefinders. In compact systems, the active material is often co-doped with Yb to enhance absorption efficiency. Investigations of spectroscopic properties and energy transfer processes between the rare earth ions in different host materials and under different conditions advance knowledge around these eye-safe 1.5 μm lasers.

In Er-doped systems, since the lower laser level is the ground state, it is necessary to excite ~50% of the Er ions in order to obtain population inversion. Therefore, a low Er dopant concentration is essential to keep thresholds low. To still obtain high absorption, a large amount of Yb<sup>3+</sup> sensitizing ions should be added to the laser medium.

Yb → Er migration-assisted non-radiative energy transfer then excites the <sup>4</sup>I<sub>11/2</sub> Er level, as illustrated in Fig. 1.

For efficient population of the <sup>4</sup>I<sub>13/2</sub> Er upper laser level via Yb ions two indispensable conditions have to be fulfilled. First, rapid excitation relaxation from <sup>4</sup>I<sub>11/2</sub> to <sup>4</sup>I<sub>13/2</sub> Er level is necessary. Otherwise reverse energy transfer to Yb ions in combination with the up-conversion processes will compete with the upper laser level population process. This may lead to lowered laser efficiency, or even inhibit 1.5 μm lasing completely. Second, the quantum yield of the upper laser level <sup>4</sup>I<sub>11/2</sub> luminescence should be high. This means that the luminescent lifetime should be close to the radiative lifetime. Both conditions are well satisfied in phosphate glasses where Er<sup>3+</sup> ion luminescent lifetimes are τ<sub>1</sub> ~ 7.5 ms for the <sup>4</sup>I<sub>11/2</sub> level and τ<sub>2</sub> ~ 1–3 μs for the <sup>4</sup>I<sub>13/2</sub> level. These two factors make Er, Yb doped phosphate glass an efficient 1.5 μm laser medium. The main drawback of the glass as a laser host in comparison to crystals is the low (~0.8 W/(K m)) thermal conductivity. Low thermal conductivity leads to low thermal damage threshold and thus limits the average output power.

As for the crystals, the search for a crystalline Er,Yb activated laser host that meets the two above-mentioned demands well is still in progress. Investigations have been

\* Corresponding author. Tel.: +46 85537 8148; fax: +46 85537 8216.  
E-mail addresses: [denker@Lst.gpi.ru](mailto:denker@Lst.gpi.ru) (B. Denker), [jh@laserphysics.kth.se](mailto:jh@laserphysics.kth.se) (J.E. Hellström).

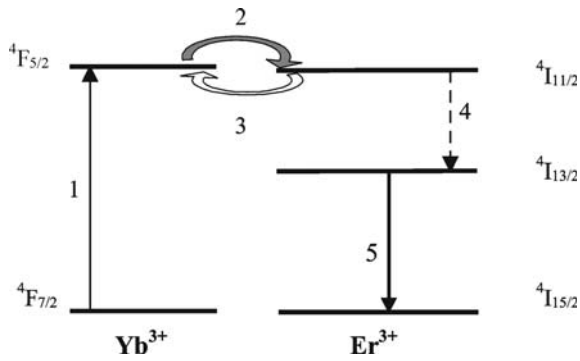


Fig. 1. The principal energy level scheme and the energy transformation processes in Yb–Er doped media. 1 – optical pumping into the Yb absorption band; 2, 3 – direct and reverse Yb–Er energy transfer; 4 – multiphonon relaxation; 5 – lasing transition.

made using e.g. YAG [1],  $\text{Y}_2\text{SiO}_5$  [2],  $\text{Ca}_2\text{Al}_2\text{SiO}_7$  [3],  $\text{YVO}_4$  [4],  $\text{YCa}_4\text{O}(\text{BO}_3)_3$  [5],  $\text{GdCa}_4\text{O}(\text{BO}_3)_3$  [6] and  $\text{KY}(\text{WO}_4)_2$  [7] crystals but glass still remains the most efficient host material. The main reason for this is the fact that all these crystalline materials have less suitable  $\tau_1$ ,  $\tau_2$  lifetimes. For example, in room-temperature YAG the lifetime  $\tau_2$  is  $\sim 100 \mu\text{s}$  which is almost two orders of magnitude longer than in phosphate-based glasses. As a result, reverse energy transfer and up-conversion make inversion at  $1.54 \mu\text{m}$  transition impossible. Lasing was obtained only at the transitions terminating at the higher Stark components of the ground  $^4\text{I}_{15/2}$  level ( $\lambda = 1.61, 1.64 \mu\text{m}$ ) [1] as they require sufficiently lower upper laser level  $^4\text{I}_{11/2}$  population to reach inversion. It should be noted that these wavelengths are off the sensitivity peak of the available Ge and InGaAs photodetectors.

At room temperature the  $\tau_2$  parameter in Er:YAG is determined by non-radiative multiphonon relaxation (MPR) while  $\tau_1$  is determined by spontaneous emission. The same is true for silicates as well as in  $\text{YVO}_4$  and  $\text{KY}(\text{WO}_4)_2$  crystals. Unfortunately the MPR rate in all these materials is not enough for irreversible Yb–Er energy transfer.

In the borate crystals, to the opposite, the MPR is too big for Yb–Er laser action. The  $^4\text{I}_{11/2}$   $\text{Er}^{3+}$  level is quenched very strongly ( $\tau_2 < 1 \mu\text{s}$ ) so that no reverse energy transfer can take place, but the upper laser level  $^4\text{I}_{13/2}$  is also seriously quenched ( $\tau_1 \sim 1 \text{ms}$ ). This results in high lasing threshold in these materials.

The spontaneous relaxation process is relatively independent on temperature while the multiphonon relaxation process is strongly dependent on temperature. The single-frequency model [8] gives the following expression for the multiphonon quenching rate  $\omega$ :

$$\omega = \omega_0 \left( \frac{\exp(E_{\text{ph}}/kT)}{\exp(E_{\text{ph}}/kT) - 1} \right)^p. \quad (1)$$

Here  $\omega_0$  is the relaxation rate at zero-temperature,  $E_{\text{ph}}$  is the energy of the highest-frequency phonons in the lattice

whose energies times  $p$  matches the band gap,  $k$  is the Boltzmann constant and  $T$  is the absolute temperature.

This indicates that a temperature increase of such crystals as YAG, vanadate or silicate crystals may be used for improving  $\tau_2$  parameter without influencing  $\tau_1$  significantly. In the present paper we have focused at YAG as a material with the best mechanical strength and thermal conductivity.

It should further be noted that though the thermal conductivity in YAG at  $800^\circ\text{C}$  drops about 3 times in comparison to room temperature, the reported value of  $\sim 0.05 \text{ W}/(\text{K cm})$  [9] remains an order of magnitude higher than that of glass. Thus if it is practically possible to realize such a hot laser medium, the benefit in comparison with Yb,Er-doped bulk glasses can be much higher thermal damage threshold and in comparison with Er-doped glass fiber lasers the suitability for high peak power pulsed regimes. Thus Er,Yb:YAG at high temperature is interesting to investigate as a potential active material for three-level  $\sim 1.54 \mu\text{m}$  lasers. However,  $\sim 1.6 \mu\text{m}$  quasi-four-level lasing will be impossible at high temperature due to thermal population of the higher Stark components of the  $^4\text{I}_{15/2}$  level. Of course, the three-level nature of the  $1.54 \mu\text{m}$  system should increase the lasing threshold compared with  $1.6 \mu\text{m}$  systems. Generally speaking, however, the high-temperature solid-state laser operation regime is not an artificial or impractical thing. For example, the active zone temperature of continuously diode pumped Yb–Er glass microchip lasers can reach hundreds of degrees centigrade. It may even result in active element local melting [10].

The main objective of this phase of our work was the study of  $\text{Yb} \rightarrow \text{Er}$  energy transfer in Er,Yb:YAG crystal and its' spectroscopic properties at high temperatures. It should be noted that the present investigation deals with low level of erbium population only and does not include the description of nonlinear (up-conversion) processes that should be influential at the high Er population levels that are required for laser action.

## 2. The crystal samples and experimental methods

The Er:YAG, Yb:YAG and Er,Yb:YAG samples used for spectroscopic investigations were prepared by the vertical zone melting method using optical heating. The following crystals were investigated:

- $2 \times 10^{20} \text{ cm}^{-3}$  Er:YAG singly-doped sample.
- $1.38 \times 10^{20} \text{ cm}^{-3}$  (1 at.%) Yb:YAG singly-doped sample.
- $0.97 \times 10^{20} \text{ cm}^{-3}$  Er:  $x \times 10^{20} \text{ cm}^{-3}$  Yb:YAG co-doped samples with  $x = 4.7, 9.7, 14$  and  $17$ .
- $0.69 \times 10^{20} \text{ cm}^{-3}$  Er:  $x \times 10^{20} \text{ cm}^{-3}$  Yb:YAG co-doped samples with  $x = 9.7, 14$  and  $17$ .
- $0.49 \times 10^{20} \text{ cm}^{-3}$  Er:  $x \times 10^{20} \text{ cm}^{-3}$  Yb:YAG co-doped samples with  $x = 9.7, 14$  and  $17$ .
- $0.34 \times 10^{20} \text{ cm}^{-3}$  Er:  $17 \times 10^{20} \text{ cm}^{-3}$  Yb:YAG co-doped sample.

For high-temperature measurements the samples were placed into a home-made resistant heated ceramic tube oven with open ends. The temperature was controlled by a thermocouple. The absorption spectra were measured using an incandescent lamp, a Ge photodiode and a grating monochromator in a single-beam scheme. Emission spectra were measured using similar optical arrangement under 975 nm laser diode excitation.

Most lifetime measurements have been done using short pulse ( $\sim 30 \mu\text{s}$ ) laser diode excitation. At high temperatures (400–800 °C) the  $\tau_2$  measurements accuracy dropped due to thermal radiation and  $\tau_2$  decrease. In this temperature range the absorption of Q-switched ruby laser radiation by the  ${}^4\text{F}_{9/2}$  Er level was found enough for accurate measurements. Due to the high luminescence quantum yield in the  $\text{Yb}^{3+} {}^2\text{F}_{5/2}$  level lifetime measurements, these measurements were held in small crystal samples ( $<0.3 \text{ mm}$ ) immersed in glycerin to avoid the possible reabsorption effect.

### 3. The results

The results of the lifetime measurements ( $\tau_1$ ,  $\tau_2$  as well as the  $\text{Yb}^{3+} {}^2\text{F}_{5/2}$  level lifetime in single-doped crystals) are presented in Fig. 2. It can be seen from Fig. 2 that neither the  $\text{Yb}^{3+} {}^2\text{F}_{5/2}$  level lifetime nor the  $\text{Er}^{3+}$  upper laser level lifetime  $\tau_1$  are significantly temperature influenced in the investigated temperature range. In contrast to this,  $\tau_2$  drops about twice with every 200 °C above room temperature. In the temperature range 600–800 °C the  $\tau_1$ ,  $\tau_2$  parameters of Er ions in YAG, as well as  $\text{Yb}^{3+}$  lifetime, become comparable with corresponding room-temperature parameters in phosphate based laser glasses.

To make a rough comparison of this statement with theoretical predictions, the band gap can be approximated as  $3750 \text{ cm}^{-1}$  [11], which can be bridged by five phonons around  $750 \text{ cm}^{-1}$ , which are available in YAG [12]. Using  $100 \mu\text{s}$  as the lifetime at room temperature, Eq. (1) then

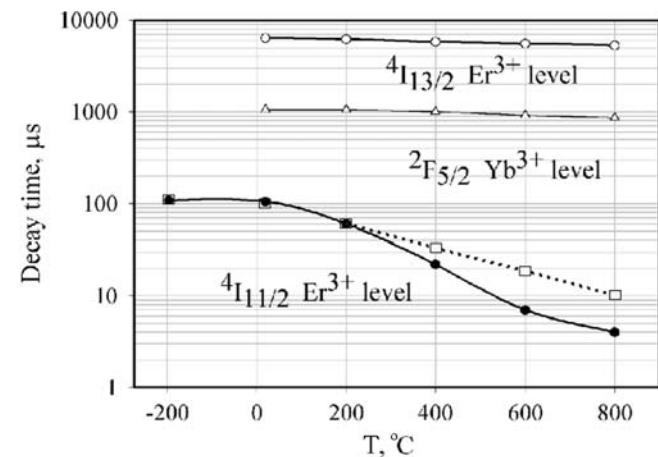


Fig. 2. Temperature dependencies of  $\text{Yb}^{3+}$  and  $\text{Er}^{3+}$  excited states lifetimes. The squares correspond to the theoretical values for the  ${}^4\text{I}_{11/2}$   $\text{Er}^{3+}$  level according to Eq. (1).

gives predictions for the lifetimes at  $-200 \text{ }^\circ\text{C}$  degrees ( $115 \mu\text{s}$ ) and  $+200 \text{ }^\circ\text{C}$  degrees ( $62.5 \mu\text{s}$ ) that correspond well with the measurements. However, at higher temperatures there is a significant discrepancy and at  $800 \text{ }^\circ\text{C}$  the single-frequency model predicts a value of  $10 \mu\text{s}$  while the measurements give a value close to  $4 \mu\text{s}$ . The reason might be an increased influence of additional relaxation processes involving lower-energy phonons omitted in the single-frequency model.

The next step of our investigation was the measurements of Yb and Er absorption and emission spectra in YAG at elevated temperatures. Measured absorption and emission spectra of  $\text{Yb}^{3+}$  and  $\text{Er}^{3+}$  in the singly-doped samples are presented in Figs. 3 and 4, respectively. Yb absorption spectrum is significantly widened at  $800 \text{ }^\circ\text{C}$  in comparison to room temperature. At  $800 \text{ }^\circ\text{C}$ , in contrast to room temperature, Yb ions in YAG even exhibit noticeable ( $\sim 0.2 \text{ cm}^{-1}$ ) absorption at  $1.06 \mu\text{m}$ . This should make it possible to pump Er,Yb:YAG by neodymium lasers in the same way as Er,Yb: glass can be pumped at room temperature.

Erbium emission spectrum in YAG at  $800 \text{ }^\circ\text{C}$  is also seriously widened in comparison to the room temperature one. The high temperature spectrum has no sharp narrow peaks at  $1.61, 1.64 \mu\text{m}$  corresponding to transitions to the upper Stark components of the  ${}^4\text{I}_{15/2}$  manifold. The main peak at  $1.54 \mu\text{m}$  is substantially widened but the emission cross-section remains significant ( $5\text{--}6 \times 10^{-21} \text{ cm}^2$ ) – again a value close to that in glass at room temperature.

The resulting gain curves for different population inversions are given in Fig. 5. It is evident that the lasing threshold will be increased since a population inversion of 0.6 seems necessary to give noticeable gain at  $800 \text{ }^\circ\text{C}$ , as opposed to 0.4 at room-temperature. The reason for this is the increased thermal population of the higher order Stark levels. Consequently, while lasing is expected to start in one of the two peaks above  $1600 \text{ nm}$  at room-temperature, due to low reabsorption loss, this is not the case at  $800 \text{ }^\circ\text{C}$ . Instead the gain spectrum becomes quite broad

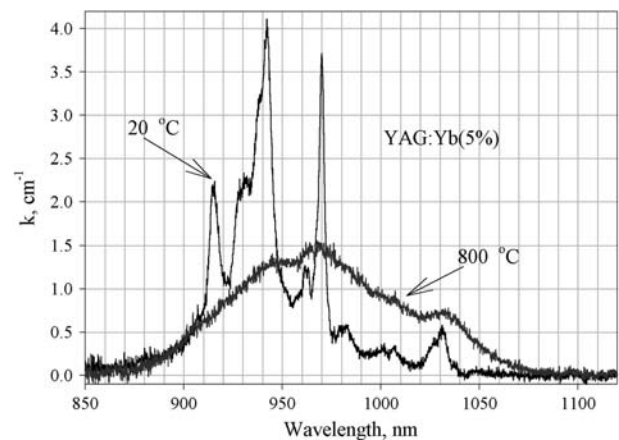


Fig. 3. Yb:YAG absorption spectra at  $20 \text{ }^\circ\text{C}$  and  $800 \text{ }^\circ\text{C}$ . Yb concentration is  $1.38 \times 10^{20} \text{ cm}^{-3}$ .

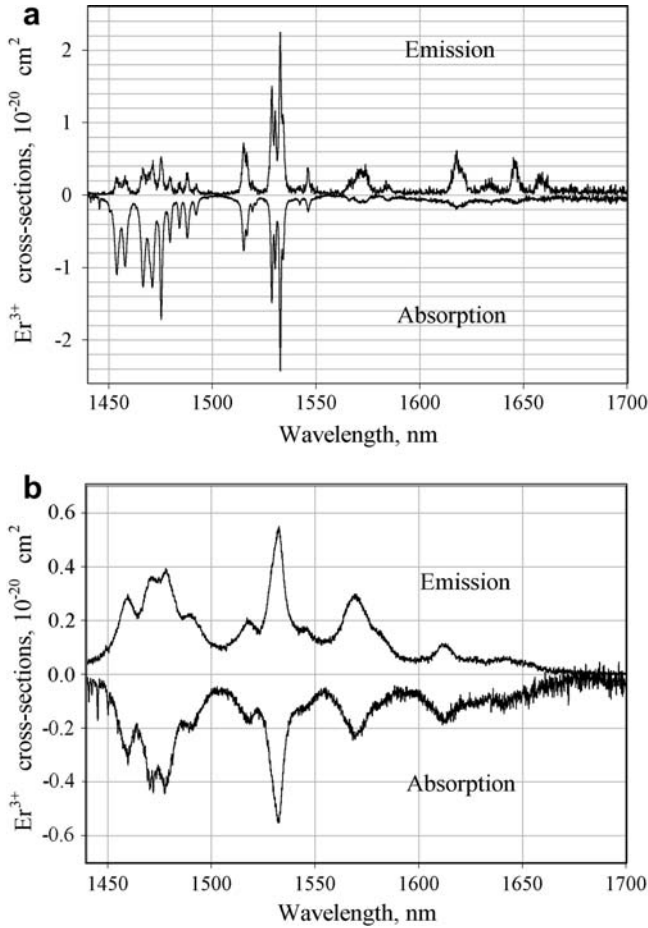


Fig. 4. Er:YAG emission and absorption spectra at 20 °C (a) and 800 °C (b).

between 1450 and 1600 nm. It follows that once the elevated threshold is reached, the emission of the 800 °C crystal should be widely tunable and have excellent properties for broadband amplification. A drawback, however, is that the reduced emission cross-sections give a reduced gain. In fact, the gain in a 3 mm long crystal at 800 °C is comparable to the gain in a 1 mm long crystal at room-temperature.

The next investigation stage was the measurements of the Yb–Er energy transfer kinetics in Er,Yb co-doped crystals at various temperatures. To avoid the possible reabsorption effect in samples with relatively high (>50%) Yb luminescence quantum yield, room-temperature measurements were held in small crystal samples (<0.5 mm) immersed in glycerin. In high-temperature measurements no immersion was used as it was found out that Yb<sup>3+</sup> luminescence quantum yield drops abruptly. The diode laser excitation pulse at 975 nm had a duration of 30 μs in these measurements. Practically in all cases (with the exception discussed below) the decay curves were pure exponential. Thus the Yb–Er energy transfer rate was defined by the formula  $W(T) = 1/\tau_e - 1/\tau_0$  where  $\tau_e$  is the temperature dependent e-fold Yb lifetime in Yb,Er co-doped sample and  $\tau_0$  is likewise the temperature dependent Yb lifetime in an Er-free sample. Fig. 6 presents several  $W$  dependen-

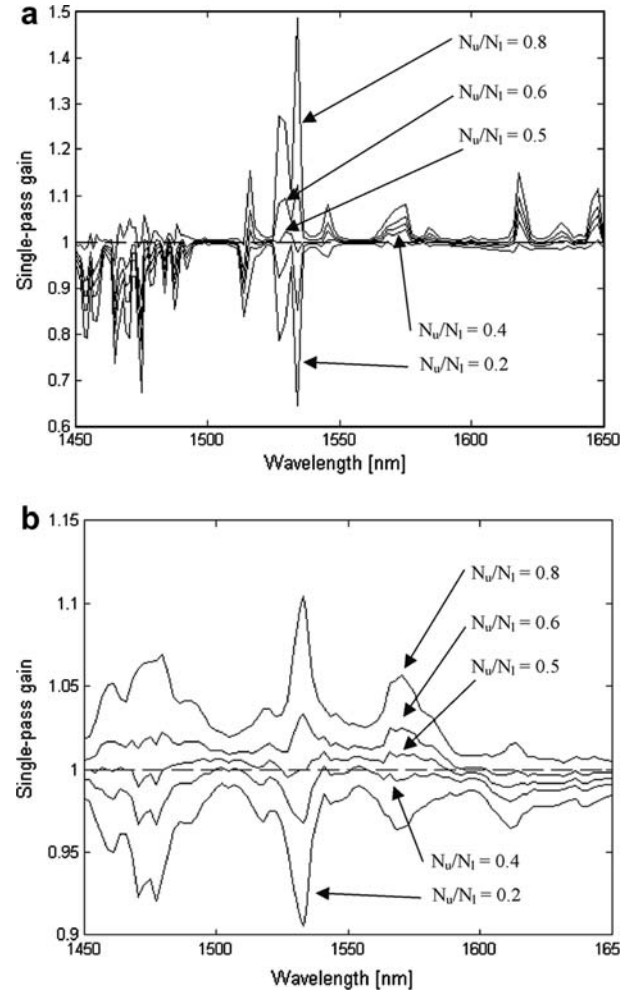


Fig. 5. Calculated gain curves for Er<sup>3+</sup> in YAG at different population inversions ( $N_u/N_i$ ) and at 20 °C (a) and 800 °C (b). Er concentration is 10<sup>20</sup> cm<sup>-3</sup> and the crystal lengths are 3 mm.

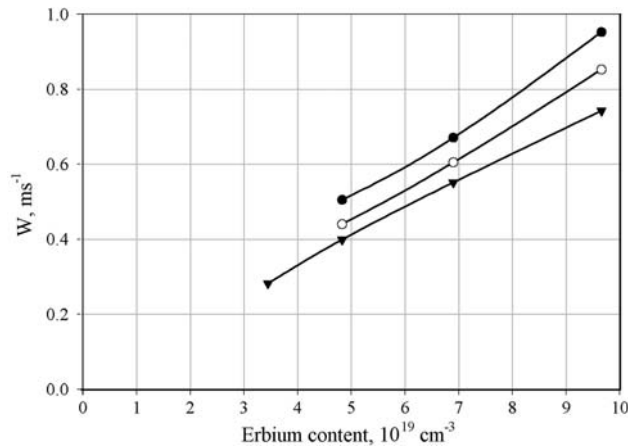


Fig. 6. The  $W$  dependencies on Er concentration at room-temperature. Solid circles refer to 9.7 × 10<sup>20</sup> cm<sup>-3</sup> Yb concentration, empty circles to 13.8 × 10<sup>20</sup> cm<sup>-3</sup> Yb concentration and solid triangles to 17.25 × 10<sup>20</sup> cm<sup>-3</sup> Yb concentration.

cies on Er content in samples with constant Yb content at room temperature. It is clearly seen that the energy transfer rate is directly proportional to the erbium concentration.

The  $W$  dependencies on Yb concentration are substantially more complicated. Fig. 7 presents an example of such dependence in samples with a fixed Er concentration of  $9.7 \times 10^{19} \text{ cm}^{-3}$ . It appears that there is no monotonous increase in Yb  $\rightarrow$  Er energy transfer rate with increasing Yb concentration as is the case in laser glasses. One can see that there is a definite optimum in Yb concentration which shifts slightly towards higher values with rising temperature. Judging from Fig. 7, it seems that, for  $0.97 \times 10^{20} \text{ cm}^{-3}$  Er concentration, the optimal Yb concentration is  $1\text{--}1.4 \times 10^{21} \text{ cm}^{-3}$  within the temperature range of 600–800 °C.

As for the absolute value of energy transfer rate, Fig. 7 shows that  $W$  increases strongly with temperature and at 600–800 °C an energy transfer quantum yield ( $\eta_{\text{Yb-Er}} = 1 - \tau_e/\tau_0$ ) of  $\sim 80\%$  can be provided in samples with  $\sim 10^{20} \text{ cm}^{-3}$  Er. Here  $\tau_e$  is the Yb lifetime in the Er co-doped sample and  $\tau_0$  is the corresponding lifetime in singly-doped Yb:YAG.

Another effect of the temperature influence on the Yb luminescence kinetics in Yb,Er co-doped samples could be reliably observed only at the highest temperature  $\sim 800$  °C. Fig. 8 presents an example of Yb luminescence kinetics in a sample with  $9.7 \times 10^{19} \text{ cm}^{-3}$  Er and  $14 \times 10^{20} \text{ cm}^{-3}$  Yb concentrations at various excitation pulse durations (30, 500 and 3000  $\mu\text{s}$ ). In about 400  $\mu\text{s}$  after the end of the pump pulse, the “usual” exponential kinetics “drags out” and transforms into another exponent of the millisecond time scale. This effect is especially well observed in the case of long pulse durations. All three kinetic curves presented in Fig. 8 are well approximated by a sum of two exponents with the e-fold times 150–160  $\mu\text{s}$  and 4.3–4.8 ms.

The reason for this phenomena is related to the thermal population of the  $^4\text{I}_{11/2}$  level from the  $^4\text{I}_{13/2}$  level. At room-

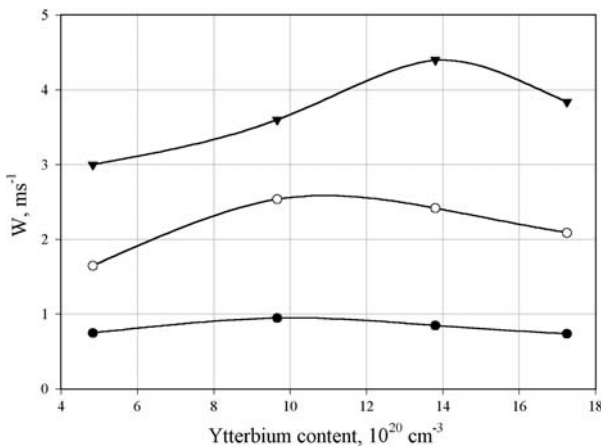


Fig. 7. The  $W$  dependencies on Yb concentration at various temperatures. Erbium content is constant,  $0.97 \times 10^{20} \text{ cm}^{-3}$ . Solid triangles refer to 800 °C measurements, empty circles to 600 °C measurements and solid circles to 20 °C measurements.

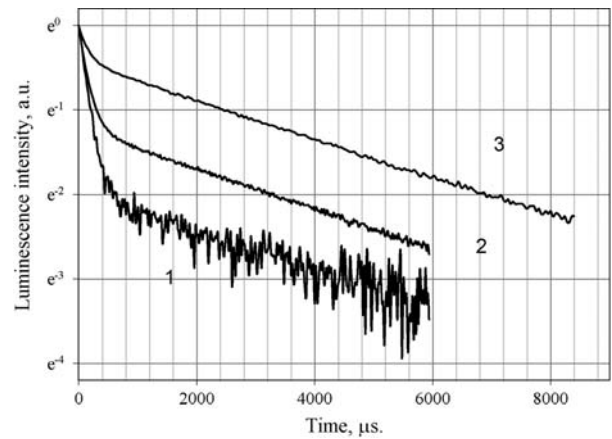


Fig. 8. Yb luminescence kinetics at 800 °C for various pump pulse durations. 1 refer to 30  $\mu\text{s}$ , 2 refer to 500  $\mu\text{s}$  and 3 refer to 3000  $\mu\text{s}$ .

temperature, the Boltzmann factor giving the ratio between the equilibrium populations of the  $^4\text{I}_{11/2}$  level and the  $^4\text{I}_{13/2}$  level is  $\sim 10^{-8}$  while at 800 °C it becomes approximately  $6 \times 10^{-3}$ . It follows, that once the initial relaxation from the  $^4\text{I}_{11/2}$  level has populated the  $^4\text{I}_{13/2}$  level significantly, there is a thermal population of the  $^4\text{I}_{11/2}$  level that decays at the same rate as the  $^4\text{I}_{13/2}$  level. Apparently, at long excitation pulse durations, the population of the upper laser level becomes large enough for the thermal mechanism of the  $^4\text{I}_{11/2}$  level population to dominate. Note that this thermal population also couples with the  $^2\text{F}_{5/2}$  level in Yb through resonant energy transfer. Due to these two processes the lifetime of the upper laser level decreases. This was measured in our experiments to give a lifetime reduction from 5.3 ms to 4.8 ms.

#### 4. Conclusion

The results obtained show that spectroscopic properties of Er,Yb:YAG at high (600–800 °C) temperatures differ radically from the room-temperature properties. There is a substantial decrease in the phonon-limited  $^4\text{I}_{11/2}$  Er<sup>3+</sup> lifetime that is significantly stronger than predicted by the single-frequency model. Actually, many of the key parameters such as  $^4\text{I}_{11/2}$  and  $^4\text{I}_{13/2}$  Er<sup>3+</sup> lifetimes and Yb<sup>3+</sup>–Er<sup>3+</sup> energy transfer rate, become comparable with that of Er,Yb laser glasses at normal conditions, a fact that could even make high-temperature YAG a potential host for three-level 1.54  $\mu\text{m}$  lasers. In order to evaluate the possibility of such lasing it is required to study the Er<sup>3+</sup> upper laser level population under high intensity pumping into Yb<sup>3+</sup> absorption band. Now this investigation as well as the high-temperature study of some other Yb–Er crystals is in progress.

#### Acknowledgments

This work was partially supported by Russian Foundation for Basic Research (Projects # 05-02-17502 and # 04-02-81015) and the Helge Ax:son Johnson Foundation.

## References

- [1] T. Schweizer, T. Jensen, E. Heumann, G. Huber, *Opt. Commun.* 118 (1995) 557.
- [2] C. Li, R. Moncorge, J. Souriau, C. Borel, C. Wyon, *Opt. Commun.* 107 (1994) 61.
- [3] B. Simondi-Teisseire, B. Viana, A.M. Lejus, J.-M. Benitez, D. Vivien, C. Borel, R. Templier, C. Wyon, *IEEE J. Quantum Electron.* 32 (1996) 2004.
- [4] N.A. Tolstik, A.E. Troshin, V.E. Kisel, N.V. Kuleshov, V.N. Matrosov, T.A. Matrosova, M.I. Kupchenko, *Advanced Solid-State Photonics 2006, Technical Digest, TuB 22*.
- [5] P.A. Burns, J.M. Dawes, P. Dekker, J.A. Piper, H. Zhang, J. Wang, *IEEE J. Quantum Electron.* 40 (2004) 1575.
- [6] B. Denker, B. Galagan, L. Ivleva, V. Osiko, S. Sverchkov, I. Voronina, J.E. Hellstrom, G. Karlsson, F. Laurell, *Appl. Phys. B* 79 (2004) 577.
- [7] N.V. Kuleshov, A.A. Lagatsky, V.G. Scherbitsky, V.P. Mikhailov, T. Jensen, A. Diening, G. Huber, *Appl. Phys. B* 64 (1997) 409.
- [8] L.A. Riseberg, H.W. Moos, *Phys. Rev.* 174 (1968) 429.
- [9] S.P. Arutyunyan, Kh.S. Bagdasarov, A.P. Dodokin, A.M. Kevorkov, *Sov. J. Solid State Phys.* 28 (1985) 957.
- [10] G. Karlsson, F. Laurell, J. Tellefsen, B. Denker, B. Galagan, V. Osiko, S. Sverchkov, *Appl. Phys. B* 75 (2002) 1.
- [11] J.B. Gruber, J.R. Quagliano, M.F. Reid, F.S. Richardson, M.E. Hills, M.D. Seltzer, S.B. Stevens, C.A. Morrison, T.H. Allik, *Phys. Rev. B* 48 (1993) 15561.
- [12] J.P. Hurrell, S.P.S. Porto, L.F. Chang, S.S. Mitra, R.P. Bauman, *Phys. Rev.* 173 (1968) 851.